Title

Palmitic acid elicits hepatic stellate cell activation through inflammasomes and hedgehog signaling

Journal

Life Sciences, 176

Author

Wu, Jian

Publication Date

2017-03-01

Peer reviewed

Life Sciences 176 (2017) 42–53

Contents lists available at ScienceDirect

Life Sciences

journal homepage: www.elsevier.com/locate/lifescie

Palmitic acid elicits hepatic stellate cell activation through inflammasomes and hedgehog signaling

Na-Na Duan [a], Xue-Jing Liu [a], Jian Wu [a,b,*]

[a] Dept. of Medical Microbiology, Key Laboratory of Molecular Virology, School of Basic Medical Sciences, Fudan University, Shanghai 200032, China
[b] Shanghai Institute of Liver Diseases, Fudan University, Shanghai 200032, China

ARTICLE INFO

Article history:
Received 16 January 2017
Received in revised form 15 March 2017
Accepted 16 March 2017
Available online 18 March 2017

Keywords:
Hepatic stellate cells
NLRP3
Hedgehog signaling
Autophagy, nonalcoholic steatohepatitis

ABSTRACT

Aims: Activation of hepatic stellate cells (HSCs) plays a pivotal role at the center of the fibrogenic progression in nonalcoholic steatohepatitis (NASH). However, it is poorly understood that how various molecules interact within HSCs during the progression of NASH to fibrosis. The aim of the present study is to delineate how inflammasome molecules, hedgehog signaling and autophagy provoke HSC activation using palmitic acid (PA) as a major insult.

Main methods: Inflammasome activation, hedgehog signaling activity and autophagy in PA-exposed HSCs were determined to investigate their role in activation of human and rodent HSC lines or primary HSCs.

Key findings: PA treatment elicited HSC activation reflected by increased mRNA levels of transforming growth factor-β1, connective tissue growth factor, tissue inhibitor of metalloproteinase-1 and procollagen type I (α1). In addition, expression levels of NOD-like receptor protein 3 (NLRP3) and hedgehog signaling transcription factor Gli-1 were increased in PA-exposed HSCs. It's evident that PA treatment resulted in increased production of light chain 3-II and autophagosomes, as well as enhanced autophagy flux reflected by transduction of an adeno-associated viral vector. Whereas, reduced autophagy, which is often seen in the late stage of NASH, provoked inflammasome activation. Moreover, suppressing the Hh signaling pathway by LDE225 blocked production of light chain 3-II and autophagy flux.

Significance: Saturated fatty acids, such as PA, stimulate HSC activation through inflammasomes and hedgehog signaling. Meanwhile, compromised autophagy may facilitate HSC activation, implicating valuable candidates for pharmacologic intervention against the progression of fibrogenesis in NASH.

1. Introduction

Twenty to 25% individuals with simple fatty liver will progress to nonalcoholic steatohepatitis (NASH) in 5–10 years [1]. Excessive accumulation of triglyceride (TG) in hepatocytes is the hallmark of NASH, and increased free fatty acid content in hepatocytes accounts for hepatocellular injury and death through oxidant stress, endoplasmic reticulum (ER) stress, insulin resistance and apoptosis or pyroptosis [2]. It has been known that hepatocellular injury and death are the initial and sustained stimuli for fibrogenesis, in which activation of hepatic stellate cells (HSCs) with a transition from a quiescent phenotype to myofibroblast-like cells is the center of the complex paradigm [3]. However, how HSCs are activated in a steatotic microenvironment, especially with increased fatty acid influx into the liver, is poorly understood. Therefore, in the present study, our intent is to investigate how fatty acids activate HSCs and the consequences using primary HSCs, human and rodent immortalized HSC lines as a platform for an initial pharmacological evaluation.

Inflammasome molecules are multiprotein complexes formed by NOD-like receptor (NLR) family members, and represent a family of recognition receptors which identify pathogen-associated molecular patterns (PAMPs) and damage-associated molecular patterns (DAMPs) in a variety of cell types [4]. Inflammasome activation has been recently recognized to play a central role in the development of carbon tetrachloride-induced and obesity-associated liver injury and fibrosis [5,6]. Among NLRs, NLRP3 senses a wide array of stimuli from the extracellular space or subcellular compartments, and participates in the process of innate immune defense. It cleaves and activates pre-caspase-1 to caspase-1, which in turn activates IL-1β and IL-18, resulting in pyroptosis [7]. However, whether inflammasomes directly affect HSC activation in a steatotic microenvironment is unknown.

The hedgehog (Hh) signaling pathway is a highly conserved cross species, and orchestrates multiple aspects of embryogenesis, development and oncogenesis [8]. Enhanced activation of the Hh signaling pathway has been shown in patients with alcoholic, non-alcoholic steatohepatitis and primary biliary cholangitis [9,10], and thought to

* Corresponding author at: Key Laboratory of Molecular Virology, Fudan University Shanghai Medical College, 138 Yixue Yuan Road, P. O. Box 228, Shanghai 200032, China.
E-mail address: jian.wu@fudan.edu.cn (J. Wu).

http://dx.doi.org/10.1016/j.lfs.2017.03.012
0024-3205/

be a key factor for cross-talk between hepatocytes and HSCs during hepatic injury and fibrosis [11,12]. However, how Hh signaling modulates HSC activation in steatohepatitis is poorly understood.

Autophagy is an intracellular pathway that breaks down damaged organelles and long-lived proteins in lysosomes to promote cell survival under various conditions, such as starvation or lipid overload [13]. It has been shown recently that autophagy mediates the breakdown of lipid droplets in hepatocytes and therefore participates in the development of hepatic steatosis [14]. Not surprisingly, intracellular droplets disappear during the process of HSC activation, which has been found to be the results of autophagy [15]. Therefore, how free fatty acids activate inflammasomes and Hh signaling in concurrence of autophagy is a crucial question in revealing the molecular basis of hepatic fibrogenesis during steatohepatitis. In this present study, we evaluate the hypothesis that activated inflammasomes and up-regulated Hh signaling participate in the activation of palmitic acid (PA)-exposed HSCs, and that autophagy interacts with these two signaling events contributing to the perplex of HSC activation.

2. Materials and methods

2.1. Sources of materials

Palmitic acid (PA, Sigma-Aldrich, St. Louis, MO), dissolving in methanol (stock solution 31.2 mM), was mixed with 5% fatty acid-free bovine serum albumin (BSA) in phosphate buffered saline (PBS) at a molar ratio of 5:1, and the final concentration was 200 μM. *S*-Adenosyl-L-methionine (SAMe), parthenolide and chloroquine (CQ) (Sigma-Aldrich, St. Louis, MO) were dissolved in distilled water, and pH of the stock solution was adjusted to 7.4. LDE225 (Cellagen Technology, CA, USA), a potent inhibitor of Smo, which is a critical transmembrane molecule in the Hh signaling pathway [16], was dissolved in dimethyl sulfoxide (DMSO) and diluted in medium. All stock solutions were kept at −20 °C till the use in experiments.

2.2. Cell culture and treatment

Three immortalized stellate cell lines were used in this study: human LX2 [17], human immortalized HSC [9] and rat BSC-C10 cells [18,19], which are partially-activated HSCs obtained separately from Drs. Scott L. Freidman, Mt. Sinai School of Medicine, New York, NY; David Brenner, University of California School of Medicine, San Diego, CA, and Hidekazu Tsukamoto, Keck School of Medicine of University of Southern California, Los Angeles, CA. Cells were cultured in DMEM with 10% fetal bovine serum (FBS, Gibco Life Technologies, Grand Island, NY), 1% (v/v) sodium pyruvate, 1% (v/v) glutamine and 1% (v/v) penicillin-streptomycin at 37 °C in 5% CO_2 and 95% air-humidified incubator. HSCs at 1×10^5 were seeded in 6-well plates for 24 h, then exposed to PA at 200 μM with or without pretreatment with SAMe (1 mM), parthenolide (5 μM), LDE225 (10 nM) or CQ (25 μM).

2.3. Quantitative reverse transcriptase polymerase chain reaction (RT-PCR) assay

Total RNA was isolated from HSCs exposed to PA with or without the preincubation with SAMe, parthenolide, LDE225 or CQ by Trizol reagent (Invitrogen, Carlsbad, California, USA) according to the manufacturer's protocols. RNA was converted to cDNA by reverse transcription using PrimeScript™ RT Reagent Kit (Takara Bio Inc., Dalian, China). qRT-PCR was performed with the Power SYBR Green PCR Master Mix (Applied Biosystems, Foster City, CA, USA). Relative gene expression was normalized to the housekeeping gene, human or rat glyceraldehyde phosphate dehydrogenase (GAPDH), and expressed as $2^{(-\Delta\Delta CT)}$ as previously described [20]. All primers were synthesized by Shenggong Biotech (Shanghai, China), and their sequences are shown in Supplemental Table 1.

2.4. Western blot analysis

Total protein was extracted with RIPA lysis buffer (Ruian BioTechnologies, Shanghai, China) and centrifuged at 12,000*g* for 15 min at 4 °C. Protein concentration was measured using a bicinchoninic acid (BCA) protein assay kit (Pierce Biotechnology, Rockford, USA). Fifty microgram of protein was subjected to sodium dodecyl sulfate polyacrylamide gel (SDS-PAGE) electrophoresis, and transferred to polyvinylidene fluoride (PVDF) membranes (Millipore, Massachusetts, USA). After being blocked with 5% BSA at room temperature (RT) for 2 h, the membranes were immunoblotted with the primary antibodies (1:500 dilutions) at 4 °C overnight, and further with horseradish peroxidase (HRP)-conjugated secondary antibodies (1:5000 dilutions). Blots were imaged using an ECL detection system (Tanon, Shanghai, China). GAPDH was used as an equal protein loading control as we reported previously [21]. All antibodies used in the experiments are shown in Supplemental Table 2.

2.5. Isolation of rat hepatic stellate cells

Animal experimental protocol was approved by the Animal Ethnic Committee of Fudan University School of Basic Medical Sciences, and all procedures follow the NIH guidelines of experimental animal handling and care. Primary HSCs were isolated from male Sprague-Dawley rats weighing about 500 g. The method of isolating primary HSC was reported previously by us [22,23]. In brief, rats were anesthetized with sodium pentobarbital intraperitoneally (60 mg/kg). After being perfused with Ca^{2+}, Mg^{2+}-free solution, pronase E and collagenase type IV (Sigma) solution, parenchymal cells were digested with DNase treatment. Finally, HSCs were separated by Nycodenz® gradient centrifugation, and cultured with M199 medium (Hyclone, Shanghai, China) containing 20% FBS and 1% penicillin-streptomycin for first 48 h, and then in M199 medium containing 10% FBS overtime.

2.6. Staining of lysosomes in HSCs

Lysotracker Red (Beyotime Biotechnology, Shanghai, China) was dissolved in M199 medium and kept at −20 °C. Primary rat HSCs were grown on coverslips (Winhongbio, Shanghai, China) for 6 days and then cultured with PA at 200 μM for 3 h. Lysotracker-red stock solution (1 μM) was added to M199 medium containing PA (37 °C) to reach a final concentration at 100 nM and co-cultured with cells for 1 h. After washing with PBS for 3 times, cells were examined under a fluorescent microscope.

2.7. Immunofluorescent staining

After treatment, HSCs on coverslips were washed twice with PBS and fixed with 4% paraformaldehyde in PBS for 15 min. Cells were blocked with 5% BSA for 1 h, and then incubated with primary anti-smooth muscle α-actin (α-SMA) or anti-LC3 antibody (1:50 in 1% BSA) at 4 °C overnight. After washing, cells were incubated with secondary fluorescein isothiocyanate (FITC)-conjugated antibody (1:50 in 1% BSA) for 1 h at 37 °C. Then cells were incubated with 4′, 6-diamidino-2-phenylindole (DAPI) for 5 min [24]. Finally, cells were examined under a confocal microscope (Leica Microsystems, Wetzlar, Germany).

2.8. mRFP-GFP-LC3 adeno-associated viral transduction for detection of autophagy flux

As autophagy is a dynamic process, the detection of LC3 processing by Western blot and visualization of autophagosome formation by fluorescent staining are insufficient to reflect autophagic activity. Therefore, we infected cells with an adeno-associated viral vector (AAV-mRFP-GFP-LC3, HanBio Technology Co. Shanghai, China), which dynamically

exhibits the autophagosome formation and lysosome degradation as an index of autophagy flux. Human HSCs at 5×10^4 were seeded in 12-well plates. When the confluency was reached to 50–70%, HSCs were exposed to AAV-RFP-GFP-LC3 at a final multiplicity of infection (MOI) of 75 in DMEM with 2% FBS at 37 °C for 24 h. Subsequently, cells were exposed to PA at 200 μM for 12 h, and micrographic images in red and green channels were recorded with a fluorescent microscope (Nikon Eclipse Ti-s, Tokyo, Japan). Autophagic flux was assessed by counting the number of GFP and RFP puncta (puncta/cell).

2.9. Statistical analysis

Experiments were repeated for at least three times. All data were presented as means ± SEM. SPSS17.0 software was used for statistical analysis. Comparisons between two groups were analyzed by unpaired Student's *t*-test, and one-way analyses of variance tests (ANOVA) followed by LSD or Dunnett T3 tests if more than two groups were included in an experimental design. p Value < 0.05 was considered to be statistically significant.

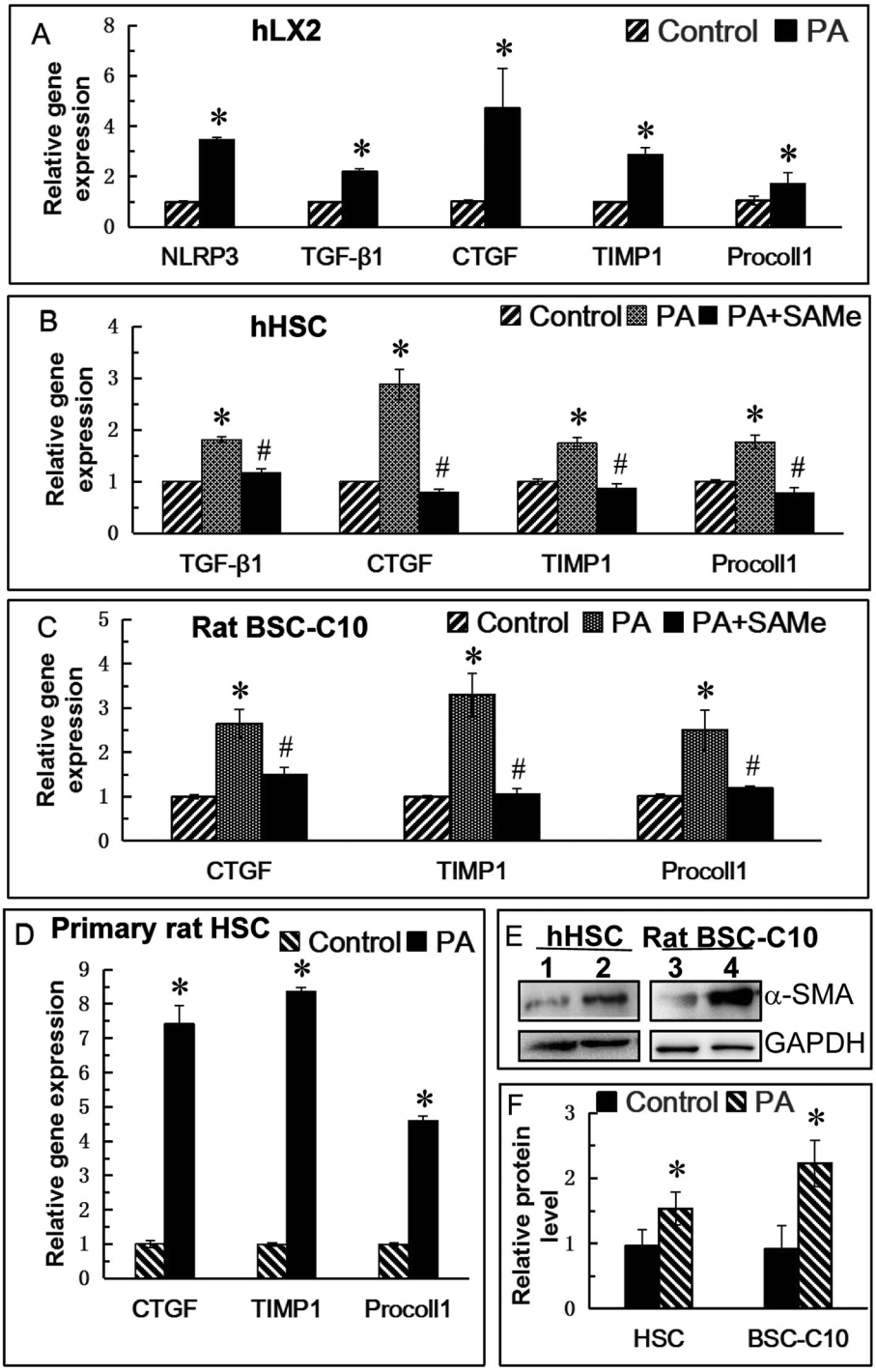

Fig. 1. PA treatment provoked HSC activation. HSCs were exposed to PA (200 μM) with or without SMAe (1 mM) for 12 h. (A–D): Gene expression levels of TGF-β1, CTGF, TIMP-1 and procollagen type I (α1) (Procoll-1). (A) Human LX2 cells; (B) Human immortalized HSCs; (C) Rat BSC-C10 cells; (D) Primary rat HSCs; (E) Protein levels of α-SMA in human immortalized HSCs and rat BSC-C10 cells. Lane 1, 3: control; Lane 2, 4: PA. *p < 0.05 compared to controls; #p < 0.05 compared to PA treatment.

3. Results

3.1. Effects of PA treatment on human LX2 cells

To investigate the role of HSCs on progression of NASH to fibrosis, we first treated LX2 cells with PA at 200 or 500 μM for 24 h, then examined gene expression levels of NLRP3 and markers of HSC activation, such as transforming growth factor-β1 (TGF-β1), connective tissue growth factor (CTGF), tissue inhibitor of metalloproteinase-1 (TIMP-1) and procollagen type I (α1) (Procoll-1) by qRT-PCR. As shown in Fig. 1A, expression levels of NLRP3, TGF-β1, CTGF, TIMP-1 and Procoll-1 genes were increased in PA-treated HSCs compared to controls, indicating that PA stimulated HSC activation in vitro, and that there was increased expression of inflammasome molecules during HSC activation.

3.2. Effects of PA on activation of human HSCs and rat BSC-C10 cells

To confirm the effect of PA on HSC activation, we repeated the experiments with primary rat HSCs and other two immortalized cell lines: human HSC and rat BSC-C10 cells. Gene expression levels of TGF-β1, CTGF, TIMP-1 and Procoll-1 in these two HSC lines were also up-regulated after exposing to PA; in contrast, SAMe, the first line of an

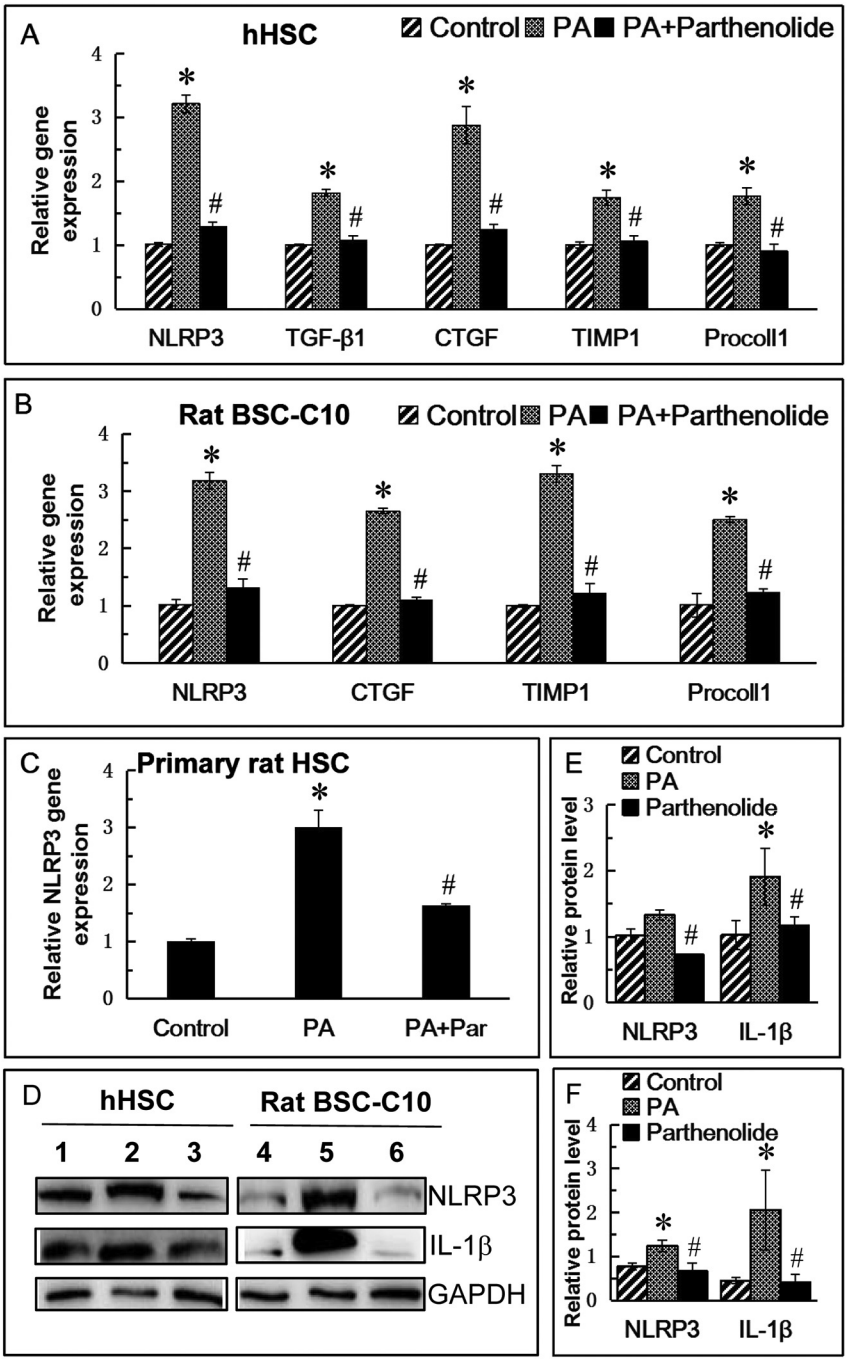

Fig. 2. PA treatment provoked HSC activation through NLRP3 activation. HSCs were exposed to PA (200 μM) with or without parthenolide (5 μM) for 12 h. (A–C): Gene expression levels of NLRP3, TGF-β1, CTGF, TIMP1 and Procoll-1. (A) Human immortalized HSCs; (B) Rat BSC-C10 cells; (C) Primary rat HSCs; (D) Protein level of NLRP3 and cleaved IL-1β in human immortalized HSCs and rat BSC-C10 cells; (E) Relative protein levels in human immortalized HSCs as evaluated by densitometric analysis; (F) Relative protein levels in rat BSC-C10 cells as evaluated by densitometric analysis. Lane 1, 4: control; Lane 2, 5: PA; Lane 3, 6: PA + Parthenolide (Par). *$p < 0.05$ compared to controls; #$p < 0.05$ compared to PA treatment.

antioxidant, neutralized oxidant stress caused by PA exposure (Fig. 1B–D). Furthermore, immunofluorescent staining confirmed that much more α-SMA, the marker of activated HSCs, was visualized in PA-treated primary rat HSCs (Fig. 4). It is obvious that treating primary rat HSCs at Day 5 after isolation with PA caused an increased deposition of α-SMA compared to untreated cells, which was consistent with the protein levels of α-SMA in immortalized human HSC and rat BSC-C10 cells (Fig. 1E,F). Therefore, it is evident that PA treatment led to HSC activation in vitro. Subsequently, we treated primary rat HSCs with PA for 8, 12 or 24 h, and it was found that the proliferative rate of primary rat HSCs was slightly increased at 12 h although the change in proliferation was not statistically significant, which was verified by immunofluorescent staining of Ki-67 (Supplemental Fig. 1A–D).

3.3. PA treatment increased expression levels of NOD-like receptor protein 3 (NLRP3)

It was shown in Fig. 2A, B, D that gene and protein levels of NLRP3 were elevated in PA-exposed HSCs. In order to further confirm whether PA-elicited HSC activation is through an inflammasome cascade, HSCs were pretreated with parthenolide, an inhibitor of inflammasomes. The results showed that parthenolide down-regulated mRNA and protein levels of NLRP3 and suppressed gene expression of TGF-β1, CTGF, TIMP-1 and Procoll-1 compared to those treated with PA alone (Fig. 2A, B, D), which were further confirmed by primary rat HSCs (Fig. 2C). Parthenolide also inhibited positivity of α-SMA in primary rat HSCs as shown in immunofluorescent staining (Fig. 4). Thus, it is

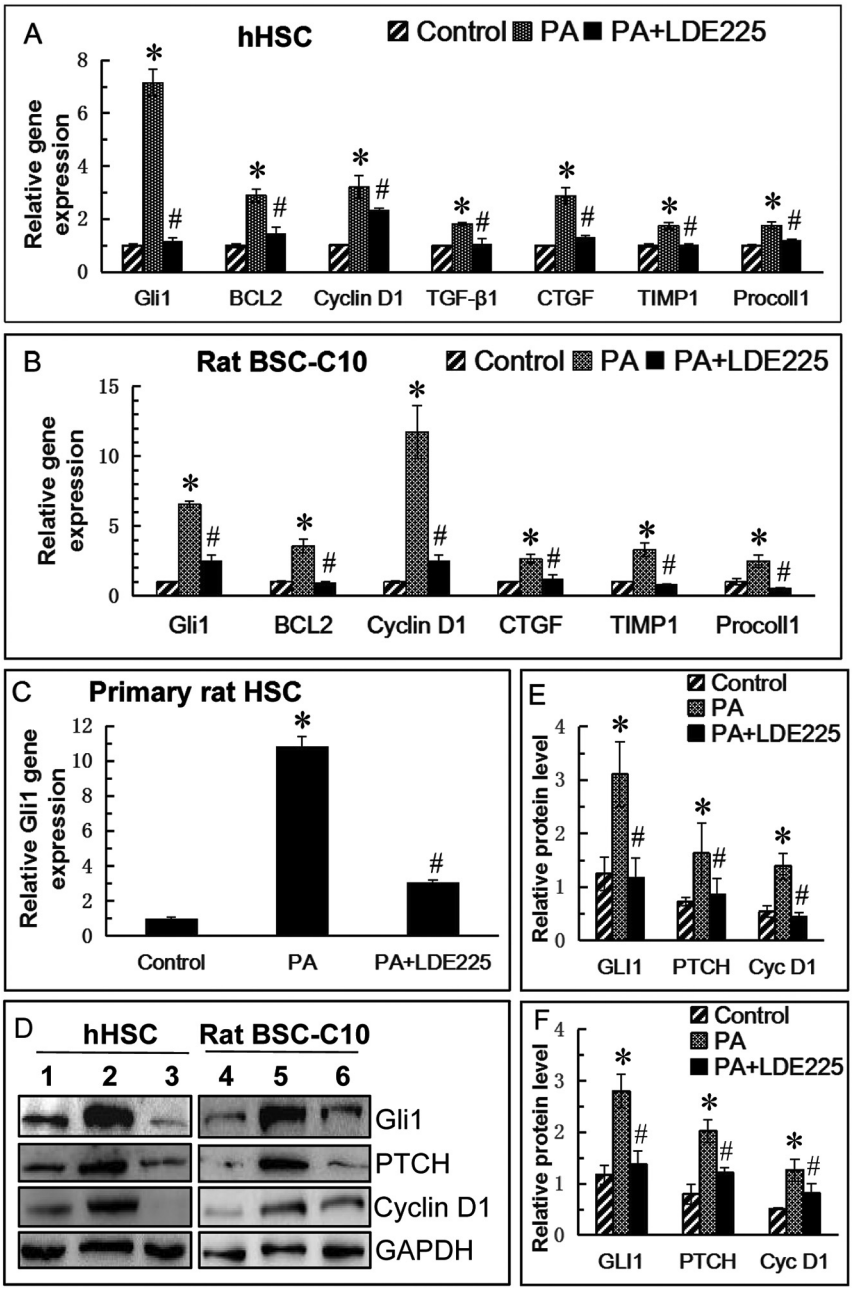

Fig. 3. PA provoked HSC activation through the hedgehog signaling pathway. HSCs were exposed to PA (200 μM) with or without LDE225 (10 nM) for 12 h. (A–C): Gene expression levels of Gli-1, cyclin D1, BCL-2, TGF-β1, CTGF, TIMP-1 and Procoll-1. (A) Human immortalized HSCs; (B) Rat BSC-C10 cells; (C) Primary rat HSCs; (D) Protein levels of PTCH, Gli-1 and cyclin D1 in human immortalized HSCs and rat BSC-C10 cells; (E) Relative protein levels in human immortalized HSCs as evaluated by densitometric analysis; (F) Relative protein levels in rat BSC-C10 cells as evaluated by densitometric analysis. Lane 1, 4: control; Lane 2, 5: PA; Lane 3, 6: PA + LDE225. *$p < 0.05$ compared to controls; #$p < 0.05$ compared to PA treatment.

conceivable that activation of inflammasome NLRP3 molecule is one of pathways for PA-elicited HSC activation. The NLRP3 activation further activated IL-1β by cleaving pre-Il-1β to its matured form (Fig. 2D, E, F). On the other hand, TdT-mediated dUTP nick end labeling (TUNEL) assay did not detect apoptosis in HSCs with PA exposure, and caspase-3 activity of rat BSC-C10 cells did not increase after PA treatment, which verified our assumption that the inflammasome activation leads to further HSC activation with an increase in the production of fibrogenic cytokines (TGF-β1 and CTGF) and extracellular matrices (TIMP-1 and Procoll-1) instead of cell death through pyroptosis or apoptosis (Supplemental Fig. 1D, E).

3.4. PA treatment increased expression levels of Gli-1

It was shown in Fig. 3A–C that the gene expression levels of Gli-1, cyclin D1 and B-cell lymphoma-2 (BCL-2), which are the downstream target genes of the Hh signaling pathway, were increased in PA-treated human immortalized HSC, rat BSC-C10 and primary rat HSC cells. In order to further confirm whether the Hh signaling pathway plays a significant role in PA-elicited HSC activation, we used LDE225 to inhibit the activity of Hh signaling. As expected, LDE225 prevented Gli-1, cyclin D1 and BCL-2 expression, and in turn inhibited expression of TGF-β1, CTGF, TIMP-1 and Procoll-1 in PA-exposed HSCs (Fig. 3A, B). Meanwhile, protein levels of PTCH, Gli-1 and cyclin D1 were suppressed in HSCs pretreated with LDE225 (Fig. 3D–F). In addition, LDE225 inhibited α-SMA level in primary rat HSCs shown by immunofluorescent staining (Fig. 4). Therefore, it appeared that PA elicited HSC activation through the Hh signaling pathway.

3.5. PA treatment provoked autophagy of HSCs

In order to explore whether autophagy plays a role in PA-elicited HSC activation, LC3-II, beclin-1 and p62, markers of autophagy, were determined at protein levels. It is apparent that ratios of LC3-II/GAPDH and beclin-1/GAPDH were elevated by PA treatment; whereas the ratio of p62/GAPDH was declined by the same treatment (Fig. 5A–C). Next,

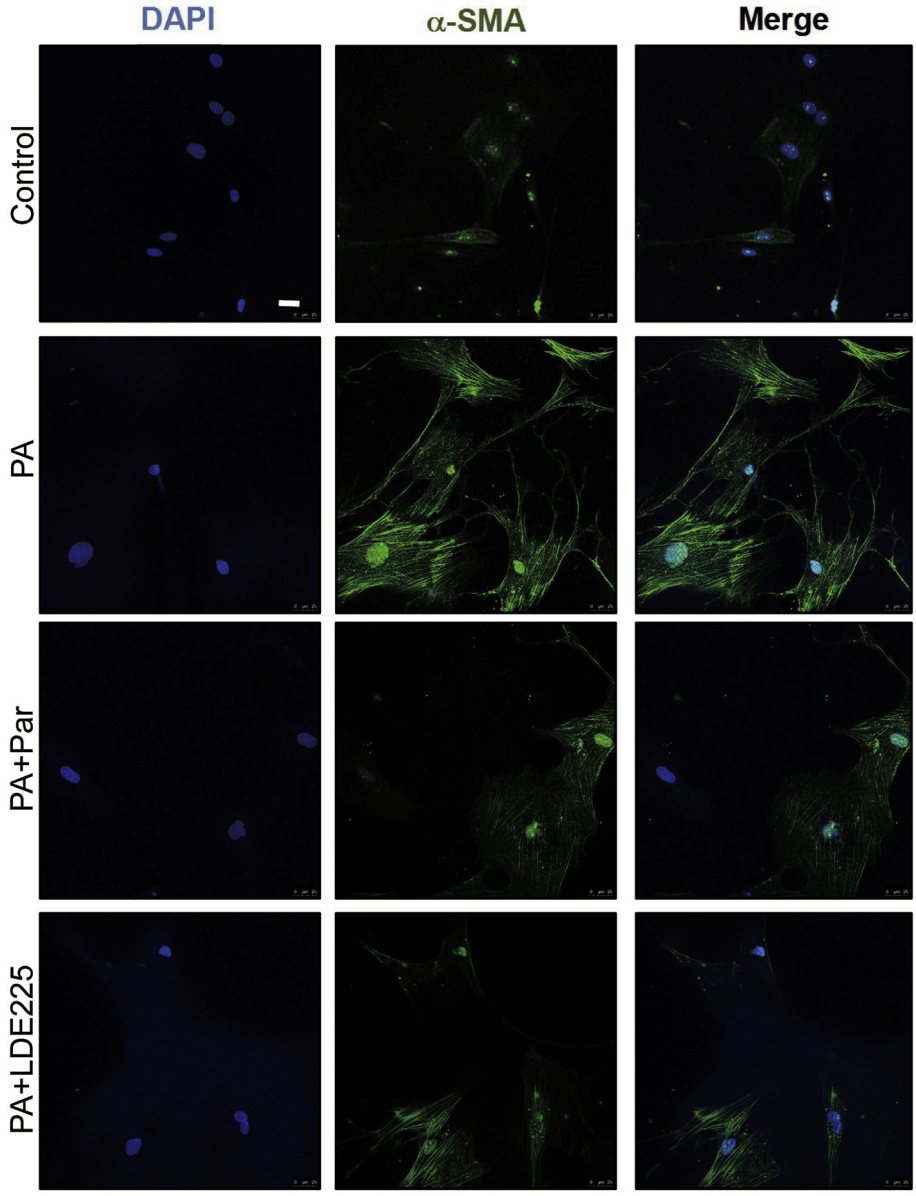

Fig. 4. Immunofluorescent staining of α-SMA in primary rat HSCs following PA treatment. Primary rat HSCs were cultured on coverslips for 5 days, and then treated with PA (200 μM) for 12 h. Thereafter, culture-activated HSC cells on slides were stained with primary and secondary antibodies as described in the Materials and Methods section. The nucleus was visualized with DAPI staining. Green: α-SMA; Blue: DAPI. Image amplification: 400×. Scale bars = 25 μm. (For interpretation of the references to color in this figure legend, the reader is referred to the web version of this article.)

HSCs were pretreated with chloroquine (CQ), an inhibitor of autophagy which suppresses the degradation of LC3B-II and p62. The results showed that protein levels of LC3-II and p62 were increased by combining PA treatment with CQ; while the expression level of beclin-1 was affected in an opposite direction (Fig. 5A–C). Therefore, it appeared that PA treatment caused a profound level of autophagy in HSCs. In order to verify these results, HSCs were infected with mRFP-GFP-LC3 adeno-associated viral vector to assess the formation of autophagosome and the degradation of LC3-II in lysosomes. In this assay, red fluorescent protein (RFP), representing the lysosome, was stable under an acidic condition; whereas green fluorescent protein (GFP), representing LC3-II, was sensitive to an acidic environment. The overlap of GFP with RFP gives rise to yellow puncta and represents the autolysosome. The results demonstrated that generation of LC3-II and autophagosome was elevated in PA-treated HSCs; whereas the formation of autophagosome in HSCs was decreased by CQ pretreatment (Fig. 6). These results further confirmed that PA treatment provoked HSC activation accompanying with enhanced autophagy. In accordance, immunofluorescent co-staining of LC3 with Lysotracker Red showed that LC3 and lysosomes were overlapped in primary HSCs with PA treatment (Fig. 5D).

3.6. The interaction between NLRP3, Gli-1 and autophagy

With the findings that NLRP3, Gli-1 and autophagy were involved in PA-elicited HSC activation, we further dissected the interaction of these two molecules with autophagy in the same experimental setting. Our results showed that expression levels of LC3-II were increased in consistence with the enhanced NLRP3 expression. Then inhibiting autophagy by CQ led to a significant increase of NLRP3 in human immortalized HSC cells (but not in BSC-C10 cells); meanwhile, CTGF and TIMP-1 levels were upregulated (Fig. 7A–D). Therefore, we speculated that inhibiting autophagy may enhance HSC activation through an inflammasome pathway during PA overload. In addition, the inhibition of Hh signaling by LDE225 decreased LC3-II levels (Fig. 7E–G), which was consistent

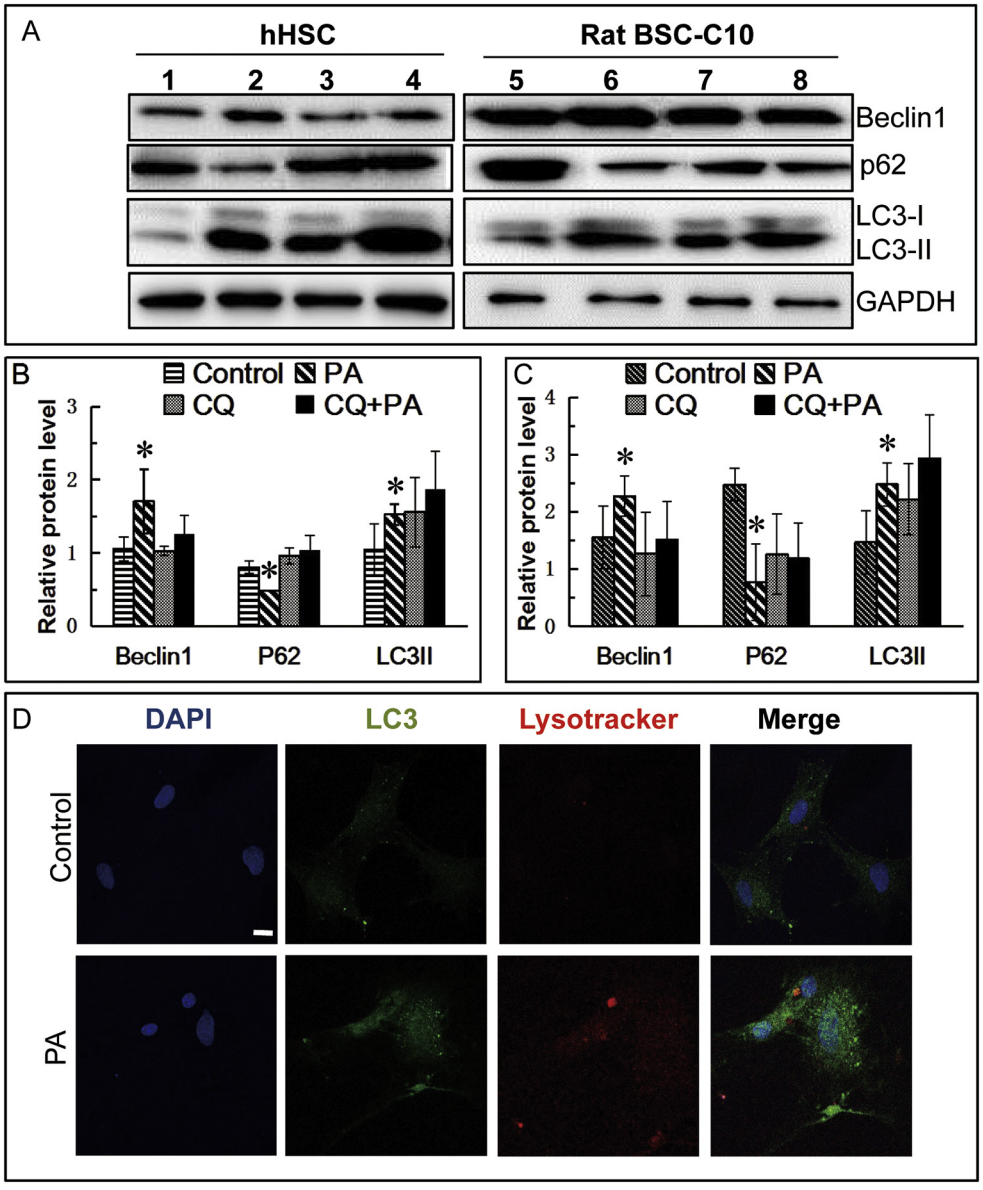

Fig. 5. PA treatment triggered autophagy in HSCs. HSCs were exposed to PA (200 μM) with or without chloroquine (CQ, 25 μM) for 12 h. (A) Protein levels of LC3-II, beclin1 and p62 in human immortalized HSCs and rat BSC-C10 cells; Lane 1, 5: control; Lane 2, 6: PA; Lane 3, 7: CQ, Lane 4, 8: PA + CQ. (B) Relative protein levels in human immortalized HSCs as evaluated by densitometric analysis; (C) Relative protein levels in rat BSC-C10 cells as evaluated by densitometric analysis; (D) The immunofluorescent staining of LC3 and Lysotracker red in primary rat HSCs. The nucleus was counter-stained with DAPI. Red: lysosome; Green: LC3-II; Blue: DAPI. *$p < 0.05$ compared with controls. Image amplification: 400×. Scale bars = 75 μm. (For interpretation of the references to color in this figure legend, the reader is referred to the web version of this article.)

with the results of AAV-mRFP-GFP-LC3 (Fig. 6). Therefore, we assumed that the Hh signaling pathway affected the development of autophagy, although exact molecular mechanisms of such an interplay remain to be investigated.

4. Discussion

Hepatic fibrosis is a pathophysiologic repairing process accompanying with chronic viral infection, alcoholism, autoimmunity or genetic abnormalities, and is an intermediate stage advancing to cirrhosis or end-stage liver disease (ESLD) that accounts for major mortality in liver diseases [25]. It has been shown that activated HSCs play a pivotal role at the center of hepatic fibrogenesis [26]. A large amount of extracellular matrix (ECM) components are produced from activated HSCs in an accelerated rate. Moreover, the production of TIMP-1 leads to a net accumulation of ECM components. Activated HSCs also release a great amount of cytokines, such as TGF-β1 and CTGF, which, in turn, affect the activation of HSCs in an autocrine fashion.

Incidence of nonalcoholic fatty liver disease (NAFLD) has been increasing in both adult and pediatric populations [27]. Understanding how NASH progresses to fibrosis and ESLD is critical for the development of therapeutics. However, the challenging for clinical practice is the lack of FDA-approved medications in the treatment of NASH. Even more unfortunate is that currently available medications in NASH

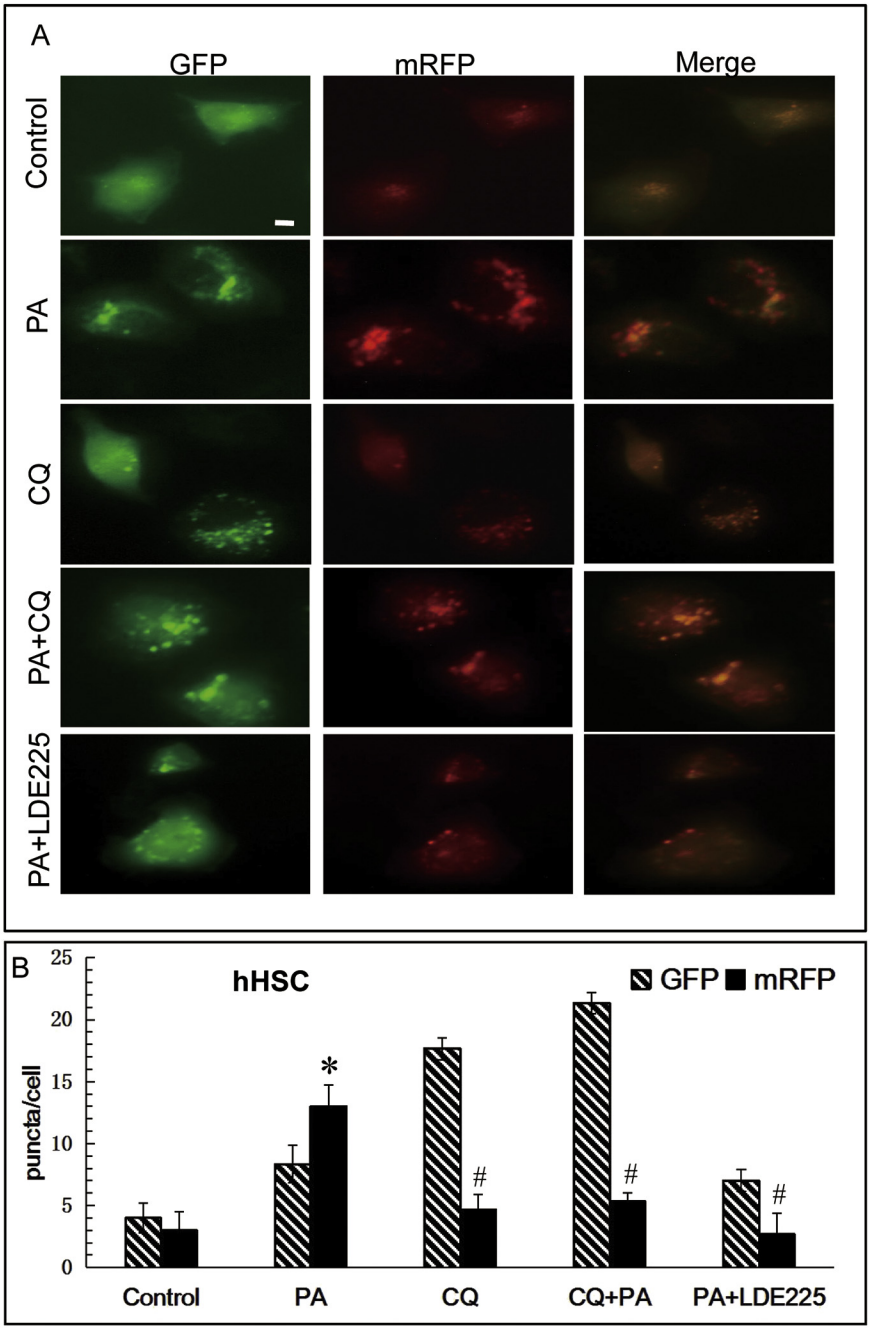

Fig. 6. Autophagic flux by transduction of AAV-mRFP-GFP-LC3 in human immortalized HSCs. When the confluency was reached to 50–70%, HSCs were infected with AAV-mRFP-GFP-LC3 at a final MOI of 100 for 24 h. Then cells were exposed to PA at 200 μM for 12 h. Autophagy was recorded with a fluorescent microscope, and representative images are shown in (A). Autophagy flux was semi-quantitatively evaluated by counting mRFP and GFP puncta number in at least 10 cells. The average puncta of per cell was used as the indication of autophagy flux (B). Green: LC3, Red: lysosome, Yellow: autophagosome. *$p < 0.05$ compared to controls, #$p < 0.05$ compared to PA treatment. Image amplification: 400×. Scale bars = 25 μm. (For interpretation of the references to color in this figure legend, the reader is referred to the web version of this article.)

treatment as suggested by practice guidelines hardly halt the progression of NASH to fibrosis [28–30]. The only promising therapeutic which has clinically been proven to have anti-fibrotic effects is a Farnesoid X receptor (FXR) agonist, obeticholic acid (OCA), which improved hepatic fibrosis in 35% NASH patients vs. 19% in those receiving placebo [29]. Moreover, reduction of endotoxin has been found to be effective in the attenuation of hepatic fibrosis in NASH patients through suppressing HSC activation and gut permeability [31]. Therefore, it is clinically demanding to reveal the molecular basis for the progression from NASH to fibrosis, and there has been an urgent need to develop therapeutics that could ameliorate steatohepatitis and block the fibrogenic process during NASH progression.

The hallmark of NASH is the increased fatty acid influx and accumulation of fatty acid content in the liver. As one of saturated fatty acids, PA was found to stimulate inflammasome NLRP3 activation in cultured Kupffer cells [32], but the results in HSCs are contradictory when different HSC lines and various concentrations were used. One study reported that PA at 75 μM led to growth rest and decrease in HSC activation [33], and another study claimed that PA at 100 μM in combination with EGF at 40 ng/mL, FGF at 220 ng/mL, oleic acid at 100 μM, and retinol at 5 μM, had a net effect of reverting HSCs to a quiescent status [34]. Whereas, in the present study, we confirmed that PA at 200 μM elicited HSC activation through the activated inflammasome NLRP3 molecule. A potent antioxidant of glutathione substrate, SAMe, abrogated PA-elicited HSC activation, indicating that oxidant stress was involved in PA-elicited HSC activation [25]. At the same time, oxidant stress is an inducer of inflammasome activation. Notably, in contrast to pyroptosis as the consequence of inflammasome activation in other cell types, such as hepatocytes, NLRP3 activation in HSCs did not result in any evidence of cell death. Although levels of cleaved IL-1β increasing, further activation and transition to myofibroblast-like cells phenotype, evidenced by increased α-SMA expression, enhanced fibrogenic cytokine release (TGF-β1 and CTGF), as well as profound extracellular matrix production (procoll-1 and TIMP-1), were seen not only in immortalized HSC lines, but also in primary HSCs, which was consistent with an early report [5]. Moreover, parthenolide [35], an inhibitor of inflammasomes, abolished PA-elicited HSC activation, cytokine release and matrix production, further indicating that inflammasome NLRP3 activation was indeed involved in PA-elicited HSC activation.

The Hh signaling pathways has been demonstrated in HSC activation in various etiologies [9–11]. Gli-1 is a transcription factor and PTCH is the receptor, both of which are the downstream target genes of the Hh signaling pathway. Hence, expression levels of Gli-1 and PTCH indirectly reflect Hh signaling activity to some extent [16]. In the present study, PA treatment led to increased Gli-1 and PTCH expression, and the use of an Hh signaling antagonist, LDE225, strikingly suppressed HSC activation, implying that inhibition of Hh signaling might abrogate PA-elicited HSC activation. Therefore, we hypothesized that the Hh

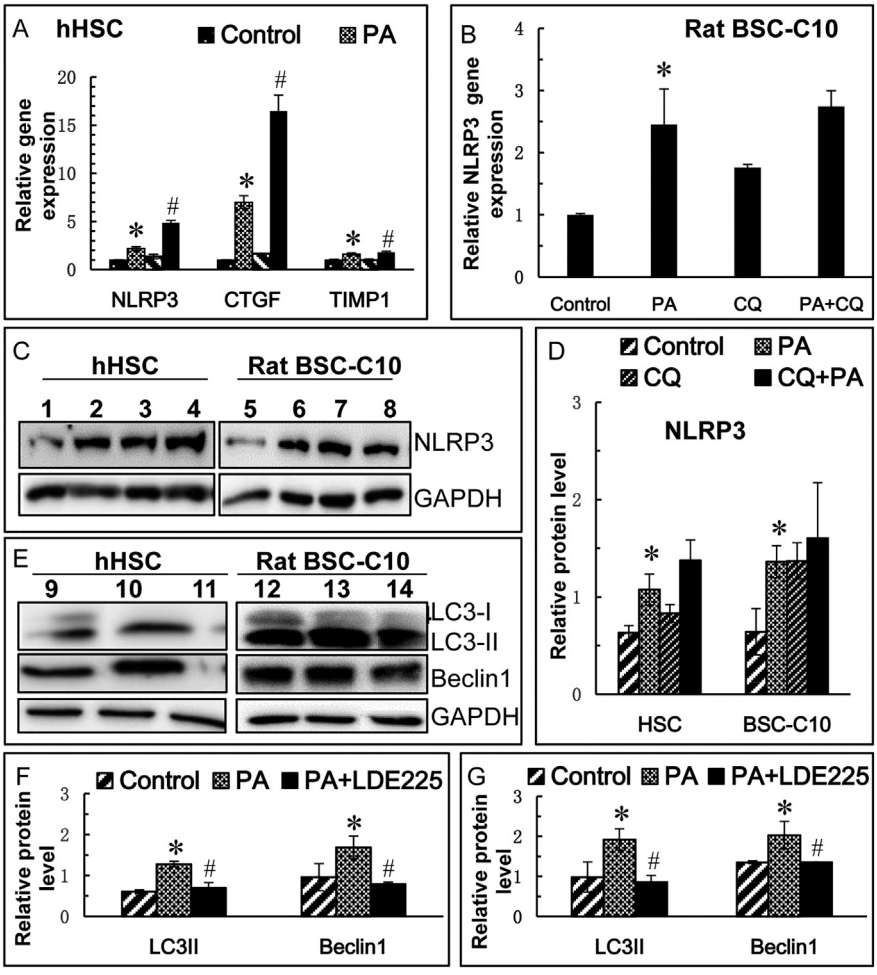

Fig. 7. Dissection of the interaction between NLRP3, Gli-1 and autophagy. (A) Inhibiting autophagy increased the gene expression of NLRP3, CTGF and TIMP-1 in human immortalized HSCs; (B) Inhibiting autophagy increased the gene expression of NLRP3 in rat BSC-C10 cells; (C) Protein levels of NLRP3 in human immortalized HSCs and rat BSC-C10 cells; (D) Relative protein levels in human immortalized HSCs and rat BSC-C10 cells as evaluated by densitometric analysis; (E) Protein levels of LC3 and beclin-1 in human immortalized HSCs and rat BSC-C10 cells; (F) Relative protein levels in human immortalized HSCs as evaluated by densitometric analysis; (G) Relative protein levels in rat BSC-C10 cells as evaluated by densitometric analysis. Lane 1,5, 9, 12: control; Lane 2, 6, 10, 13: PA; Lane 3,7: CQ; Lane 4, 8: PA + CQ; Lane 11, 14: PA + LDE225. *$p < 0.05$ compared to controls; #$p < 0.05$ compared to PA treatment.

signaling pathway was involved in the PA-elicited HSC activation. For this reason, Hh signaling inhibitors have been suggested for potential application in the treatment of NASH-associated fibrosis (vismodegib, GDC-0449) [36]. Since LDE225 (Sonidegib), which has been approved recently for the treatment of basal cell carcinoma [37], having a very high bioavailability and being efficacious at nM scale in this study, it seems to be a good candidate for clinical evaluation.

Autophagy is a physiological response for cell to clean up cellular components, such as lipids, and is involved in HSC activation. In this experiment, autophagy was triggered in human or rat immortalized HSCs evidenced by increased protein levels of beclin-1, LC3-II and decreased p62, as well as elevated autophagy flux. It is notable that blocking autophagy by CQ enhanced inflammasome NLRP3 at mRNA and protein levels in HSCs, indicating that compromised lipid autophagy (lipophagy) might result in profound lipotoxicity and HSC transition to a myofibroblast-like phenotype through inflammasome activation, although its molecular mechanisms remaining to be investigated. On the other hand, suppressing Hh signaling by LDE225 abrogated PA-provoked autophagy, probably through direct inhibition of HSC activation. This further pointed to the benefits of using LDE225 as an antifibrotic agent and warranted further investigation in animal models of NASH, regardless of molecular links between Hh signaling and autophagy having been recently characterized in other model systems [38]. In order to help understand the experimental design and the relationship of inflammasome activation, Hh signaling and autophagy in PA-elicited HSC activation, a schematic illustration is shown in Fig. 8. In the illustration, the cascades of signaling pathways and molecular interactions of these three components are highlighted, and possible molecular targets in modulating HSC activation by intervening inflammasome molecules and Hh signaling pathways or modulating the autophagy process are indicated.

In conclusion, the findings from this study demonstrated that fatty acid might directly activate HSCs through activated inflammasomes and up-regulated hedgehog signaling. Autophagy was involved in HSC activation, and compromised autophagy further activated HSCs through the inflammasome activation pathway. Suppressing inflammasome activation or Hh signaling could well be the intervention of NASH-associated fibrosis, and modulating autophagic activity may confer an option in minimizing the progression of NASH to fibrosis.

Supplementary data to this article can be found online at http://dx.doi.org/10.1016/j.lfs.2017.03.012.

Funding support

This work is supported by the Ministry of Science & Technology (#2016YFE0107400), the National Natural Science Foundation of China (NSFC #81272436 & 81572356) and Shanghai Commission of Sciences and Technologies (#16140903700) to J.W.

Author contribution

Na-Na Duan:Design and conduct experiments, collect and analyze data, and prepare manuscript.

Xue-Jing Liu: Participate in some experiments.

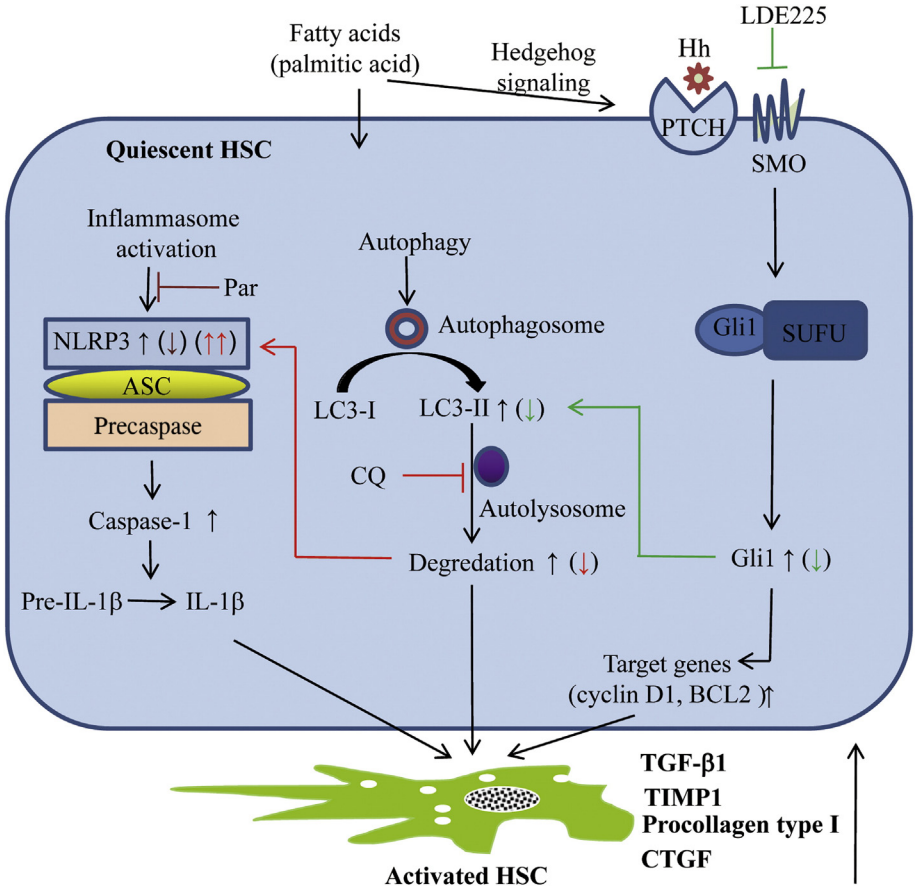

Fig. 8. Illustration of the cascades of signaling pathways and molecular interactions between inflammasome, hedgehog signaling and autophagy in PA-elicited HSC activation. PA increased the expression of NLRP3 and Gli-1 accompanying with enhanced autophagy. Inhibiting autophagy by CQ potentiated inflammation through activation of inflammasome (red arrow). Moreover, suppressing Gli-1 expression by LDE225 prevented the autophagy (green arrow). ASC: an intermediate adaptor protein to which inflammasome binds during downstream activation. CQ: chloroquine, Par: Parthenolide, CTGF: connective tissue growth factor, LC3: light chain 3, Hh: hedgehog ligands, NLRP3: NOD-like receptor protein 3, TGF-β1: transforming growth factor-β1, TIMP-1: tissue inhibitor of metalloproteinase-1. ↑ indicates upregulation, ↓ indicates downregulation. (For interpretation of the references to color in this figure legend, the reader is referred to the web version of this article.)

Jian Wu: Design experiments, analyze data, examine and approve manuscript, and supply funds.

Disclosure of conflict of interest

All authors in this manuscript declare that there is no conflict of interest associated with the work.

Abbreviations

α-SMA	smooth muscle α-actin
BrdU	5-bromo-2′-deoxyuridine
CQ	chloroquine
CTGF	connective tissue growth factor
DAMP	damage-associated molecular pattern
ECM	extracellular matrix
EMT	epithelial-mesenchymal transition
FBS	fetal bovine serum
HCC	hepatocellular carcinoma
Hh	hedgehog
HSC	hepatic stellate cell
LC3	light chain 3
BCL2	B-cell lymphoma-2
NAFLD	nonalcoholic fatty liver disease
NASH	nonalcoholic steatohepatitis
NLRP3	NOD-like receptor protein 3
PA	palmitic acid
PAMP	pathogen-associated molecular pattern
Procoll-1	procollagen type I (α1)
ROS	reactive oxygen species
SAMe	S-adenosyl-L-methionine
TG	triglyceride
TGF-β1	transforming growth factor-β1
TIMP1	tissue inhibitor of metalloproteinase-1
TUNEL	TdT-mediated dUTP nick end labeling

Acknowledgements

The authors are grateful for technical assistance from Mrs. Ke Qiao and productive discussion with Dr. Ning-Ping Zhang, Dept. of Gastroenterology, Fudan University-Affiliated Zhongshan Hospital, Shanghai, China.

References

[1] A. Suzuki, A.M. Diehl, Nonalcoholic steatohepatitis, Annu. Rev. Med. (2016)http://dx.doi.org/10.1146/annurev-med-051215-031109.
[2] A. Sahebkar, G.T. Chew, G.F. Watts, New peroxisome proliferator-activated receptor agonists: potential treatments for atherogenic dyslipidemia and non-alcoholic fatty liver disease, Expert. Opin. Pharmacother. 15 (4) (2014) 493–503.
[3] A.J. Sanyal, S.L. Friedman, A.J. McCullough, L. Dimick-Santos, D. American Association for the Study of Liver, F. United States, A. Drug, Challenges and opportunities in drug and biomarker development for nonalcoholic steatohepatitis: findings and recommendations from an American Association for the Study of Liver Diseases-U.S. Food and Drug Administration Joint Workshop, Hepatology 61 (4) (2015) 1392–1405.
[4] T. Strowig, J. Henao-Mejia, E. Elinav, R. Flavell, Inflammasomes in health and disease, Nature 481 (7381) (2012) 278–286.
[5] A. Watanabe, M.A. Sohail, D.A. Gomes, A. Hashmi, J. Nagata, F.S. Sutterwala, S. Mahmood, M.N. Jhandier, Y. Shi, R.A. Flavell, W.Z. Mehal, Inflammasome-mediated regulation of hepatic stellate cells, Am. J. Phys. Gastrointest. Liver 296 (6) (2009) G1248–G1257.
[6] J. Henao-Mejia, E. Elinav, C. Jin, L. Hao, W.Z. Mehal, T. Strowig, C.A. Thaiss, A.L. Kau, S.C. Eisenbarth, M.J. Jurczak, J.P. Camporez, G.I. Shulman, J.I. Gordon, H.M. Hoffman, R.A. Flavell, Inflammasome-mediated dysbiosis regulates progression of NAFLD and obesity, Nature 482 (7384) (2012) 179–185.
[7] D.R. Mason, P.L. Beck, D.A. Muruve, Nucleotide-binding oligomerization domain-like receptors and inflammasomes in the pathogenesis of non-microbial inflammation and diseases, J. Innate Immun. 4 (1) (2012) 16–30.
[8] L. Lum, P.A. Beachy, The Hedgehog response network: sensors, switches, and routers, Science 304 (5678) (2004) 1755–1759.
[9] C.D. Guy, A. Suzuki, M. Zdanowicz, M.F. Abdelmalek, J. Burchette, A. Unalp, A.M. Diehl, C.R.N. Nash, Hedgehog pathway activation parallels histologic severity of injury and fibrosis in human nonalcoholic fatty liver disease, Hepatology 55 (6) (2012) 1711–1721.
[10] I.S. Chan, C.D. Guy, M.V. Machado, A. Wank, V. Kadiyala, G. Michelotti, S. Choi, M. Swiderska-Syn, G. Karaca, T.A. Pereira, M.T. Yip-Schneider, C. Max Schmidt, A.M. Diehl, Alcohol activates the hedgehog pathway and induces related procarcinogenic processes in the alcohol-preferring rat model of hepatocarcinogenesis, J. Innate Immun. 38 (3) (2014) 787–800.
[11] Y. Chen, S.S. Choi, G.A. Michelotti, I.S. Chan, M. Swiderska-Syn, G.F. Karaca, G. Xie, C.A. Moylan, F. Garibaldi, R. Premont, H.B. Suliman, C.A. Piantadosi, A.M. Diehl, Hedgehog controls hepatic stellate cell fate by regulating metabolism, Gastroenterology 143 (5) (2012), 1319-29 e1-11. .
[12] G. Xie, G. Karaca, M. Swiderska-Syn, G.A. Michelotti, L. Kruger, Y. Chen, R.T. Premont, S.S. Choi, A.M. Diehl, Cross-talk between Notch and Hedgehog regulates hepatic stellate cell fate in mice, Hepatology 58 (5) (2013) 1801–1813.
[13] D.J. Klionsky, K. Abdelmohsen, A. Abe, M.J. Abedin, H. Abeliovich, A. Acevedo Arozena, Guidelines for the use and interpretation of assays for monitoring autophagy (3rd edition), Autophagy 12 (1) (2016) 1–222.
[14] A. Gonzalez-Rodriguez, R. Mayoral, N. Agra, M.P. Valdecantos, V. Pardo, M.E. Miquilena-Colina, J. Vargas-Castrillon, O. Lo Iacono, M. Corazzari, G.M. Fimia, M. Piacentini, J. Muntane, L. Bosca, C. Garcia-Monzon, P. Martin-Sanz, A.M. Valverde, Impaired autophagic flux is associated with increased endoplasmic reticulum stress during the development of NAFLD, Cell Death Dis. 5 (2014), e1179. .
[15] L.F. Thoen, E.L. Guimaraes, L. Dolle, I. Mannaerts, M. Najimi, E. Sokal, L.A. van Grunsven, A role for autophagy during hepatic stellate cell activation, J. Hepatol. 55 (6) (2011) 1353–1360.
[16] Y.H. Fan, J. Ding, S. Nguyen, X.J. Liu, G. Xu, H.Y. Zhou, N.N. Duan, S.M. Yang, M.A. Zern, J. Wu, Aberrant hedgehog signaling is responsible for the highly invasive behavior of a subpopulation of hepatoma cells, Oncogene 35 (1) (2016) 116–124.
[17] L. Xu, A.Y. Hui, E. Albanis, M.J. Arthur, S.M. O'Byrne, W.S. Blaner, P. Mukherjee, S.L. Friedman, F.J. Eng, Human hepatic stellate cell lines, LX-1 and LX-2: new tools for analysis of hepatic fibrosis, Gut 54 (1) (2005) 142–151.
[18] J.W. Kim, Y.H. Zhang, M.A. Zern, J.J. Rossi, J. Wu, Short hairpin RNA causes the methylation of transforming growth factor-beta receptor II promoter and silencing of the target gene in rat hepatic stellate cells, Biochem. Biophys. Res. Commun. 359 (2) (2007) 292–297.
[19] C.K. Sung, H. She, S. Xiong, H. Tsukamoto, Tumor necrosis factor-alpha inhibits peroxisome proliferator-activated receptor gamma activity at a posttranslational level in hepatic stellate cells, Am. J. Phys. Gastrointest. Liver 286 (5) (2004) G722–G729.
[20] J. Wu, L. Liu, R.D. Yen, A. Catana, M.H. Nantz, M.A. Zern, Liposome-mediated extracellular superoxide dismutase gene delivery protects against acute liver injury in mice, Hepatology 40 (1) (2004) 195–204.
[21] X. Chen, S. Lingala, S. Khoobyari, J. Nolta, M.A. Zern, J. Wu, Epithelial mesenchymal transition and hedgehog signaling activation are associated with chemoresistance and invasion of hepatoma subpopulations, J. Hepatol. 55 (4) (2011) 838–845.
[22] S.S. Zhan, J.X. Jiang, J. Wu, C. Halsted, S.L. Friedman, M.A. Zern, N.J. Torok, Phagocytosis of apoptotic bodies by hepatic stellate cells induces NADPH oxidase and is associated with liver fibrosis in vivo, Hepatology 43 (3) (2006) 435–443.
[23] J. Zhu, J. Wu, E. Frizell, S.L. Liu, R. Bashey, R. Rubin, P. Norton, M.A. Zern, Rapamycin inhibits hepatic stellate cell proliferation in vitro and limits fibrogenesis in an in vivo model of liver fibrosis, Gastroenterology 117 (5) (1999) 1198–1204.
[24] F. Li, Z. Song, Q. Li, J. Wu, J. Wang, C. Xie, C. Tu, J. Wang, X. Huang, W. Lu, Molecular imaging of hepatic stellate cell activity by visualization of hepatic integrin alphavbeta3 expression with SPECT in rat, Hepatology 54 (3) (2011) 1020–1030.
[25] J. Wu, M.A. Zern, Hepatic stellate cells: a target for the treatment of liver fibrosis, J. Gastroenterol. 35 (9) (2000) 665–672.
[26] S.L. Friedman, Mechanisms of hepatic fibrogenesis, Gastroenterology 134 (6) (2008) 1655–1669.
[27] Z.M. Younossi, A.B. Koenig, D. Abdelatif, Y. Fazel, L. Henry, M. Wymer, Global epidemiology of nonalcoholic fatty liver disease-meta-analytic assessment of prevalence, incidence, and outcomes, Hepatology 64 (1) (2016) 73–84.
[28] C. Conforti-Andreoni, P. Ricciardi-Castagnoli, A. Mortellaro, The inflammasomes in health and disease: from genetics to molecular mechanisms of autoinflammation and beyond, Cell. Mol. Immunol. 8 (2) (2011) 135–145.
[29] B.A. Neuschwander-Tetri, R. Loomba, A.J. Sanyal, J.E. Lavine, M.L. Van Natta, M.F. Abdelmalek, N. Chalasani, S. Dasarathy, A.M. Diehl, B. Hameed, K.V. Kowdley, A. McCullough, N. Terrault, J.M. Clark, J. Tonascia, E.M. Brunt, D.E. Kleiner, E. Doo, N.C.R. Network, Farnesoid X nuclear receptor ligand obeticholic acid for non-cirrhotic, non-alcoholic steatohepatitis (FLINT): a multicentre, randomised, placebo-controlled trial, Lancet 385 (9972) (2015) 956–965.
[30] F. Violi, R. Cangemi, Pioglitazone, vitamin E, or placebo for nonalcoholic steatohepatitis, N. Engl. J. Med. 363 (12) (2010) 1185–1186 (author reply 1186).
[31] A. Douhara, K. Moriya, H. Yoshiji, R. Noguchi, T. Namisaki, M. Kitade, K. Kaji, Y. Aihara, N. Nishimura, K. Takeda, Y. Okura, H. Kawaratani, H. Fukui, Reduction of endotoxin attenuates liver fibrosis through suppression of hepatic stellate cell activation and remission of intestinal permeability in a rat non-alcoholic steatohepatitis model, Mol. Med. Rep. 11 (3) (2015) 1693–1700.
[32] K. Miura, L. Yang, N. van Rooijen, D.A. Brenner, H. Ohnishi, E. Seki, Toll-like receptor 2 and palmitic acid cooperatively contribute to the development of nonalcoholic steatohepatitis through inflammasome activation in mice, Hepatology 57 (2) (2013) 577–589.
[33] A. Abergel, V. Sapin, N. Dif, C. Chassard, C. Darcha, J. Marcand-Sauvant, B. Gaillard-Martinie, E. Rock, P. Dechelotte, P. Sauvant, Growth arrest and decrease of alpha-SMA and type I collagen expression by palmitic acid in the rat hepatic stellate cell line PAV-1, Dig. Dis. Sci. 51 (5) (2006) 986–995.
[34] A. El Taghdouini, M. Najimi, P. Sancho-Bru, E. Sokal, L.A. van Grunsven, In vitro reversion of activated primary human hepatic stellate cells, Fibrogenesis Tissue Repair 8 (2015) 14.
[35] C. Juliana, T. Fernandes-Alnemri, J. Wu, P. Datta, L. Solorzano, J.W. Yu, R. Meng, A.A. Quong, E. Latz, C.P. Scott, E.S. Alnemri, Anti-inflammatory compounds parthenolide and Bay 11-7082 are direct inhibitors of the inflammasome, J. Biol. Chem. 285 (13) (2010) 9792–9802.

[36] A. Pratap, S. Singh, V. Mundra, N. Yang, R. Panakanti, J.D. Eason, R.I. Mahato, Attenuation of early liver fibrosis by pharmacological inhibition of smoothened receptor signaling, J. Drug Target. 20 (9) (2012) 770–782.
[37] J. Rodon, H.A. Tawbi, A.L. Thomas, R.G. Stoller, C.P. Turtschi, J. Baselga, J. Sarantopoulos, D. Mahalingam, Y. Shou, M.A. Moles, L. Yang, C. Granvil, E. Hurh, K.L. Rose, D.D. Amakye, R. Dummer, A.C. Mita, A phase I, multicenter, open-label, first-in-human, dose-escalation study of the oral smoothened inhibitor Sonidegib (LDE225) in patients with advanced solid tumors, Clin. Cancer Res. 20 (7) (2014) 1900–1909.
[38] M. Jimenez-Sanchez, F.M. Menzies, Y.Y. Chang, N. Simecek, T.P. Neufeld, D.C. Rubinsztein, The Hedgehog signalling pathway regulates autophagy, Nat. Commun. 3 (2012) 1200.